Journal of Inclusion Phenomena and Molecular Recognition in Chemistry **22:** 131–143, 1995.

Interaction of Naproxen with α-, β-, and γ-Hydroxypropyl Cyclodextrins in Solution and in the Solid State

F. MELANI[1],* G. P. BETTINETTI[2], P. MURA[1] and A. MANDERIOLI[1]
[1]*Dipartimento di Scienze Farmaceutiche, Università di Firenze, Via G. Capponi 9, 50121 Firenze, Italy.* [2]*Dipartimento di Chimica Farmaceutica, Università di Pavia, Viale Taramelli 12, 27100 Pavia, Italy*

(Received: 11 January 1995; in final form: 5 May 1995)

Abstract. Solid combinations of naproxen with amorphous hydroxypropyl derivatives of α-, β-, and γ-cyclodextrin with an average substitution degree per anhydroglucose unit of 0.6 were investigated for thermal behaviour (differential scanning calorimetry), drug crystallinity (X-ray diffractometry), and dissolution rate (dispersed amount and rotating disc methods). Phase-solubility analysis and computer-aided molecular modelling were carried out to study the inclusion complexation of naproxen with hydroxypropyl cyclodextrins. The cavity size of the host is a selective factor for the solubilizing effect, complexing ability, and dissolution rate enhancement on naproxen, hydroxypropyl β-cyclodextrin being markedly the most effective derivative. No relationship was found between the decrease in crystallinity of the drug dispersed in the amorphous carrier matrix and the geometrical features of the cyclodextrin macrocycle.

Key words. Hydroxypropyl α-, β-, or γ-cyclodextrin, naproxen, amorphous naproxen/hydroxypropyl-cyclodextrin blends, inclusion complexes, crystallinity, dissolution rate, thermodynamic parameters, molecular modelling, thermal analysis, X-ray diffraction.

1. Introduction

The very low aqueous solubility of naproxen, a nonsteroidal antiinflammatory agent, is enhanced by inclusion complexation with native, crystalline cyclodextrins, whose solubilizing potential is strongly improved by conversion in amorphous mixtures of randomly-substituted derivatives [1, 2]. We ourselves have reported that naproxen amorphization can be easily brought about in blends with amorphous methyl and hydroxyethyl derivatives of β-cyclodextrin [3–6]. It was postulated that naproxen embedded in the amorphous phase of the carrier could lose its crystallinity as a consequence of a loosening of crystal forces operating in its structure by molecular dispersion onto the surface or even by inclusion inside the cavity of the host. To shed light on the possible role of inclusion in the amorphization process, amorphous cyclodextrins with different cavity sizes and the same average

* Author for correspondence.

substitution degree per anhydroglucose unit (MS) were selected as model partners for naproxen, i.e. hydroxypropyl α-cyclodextrin MS 0.6 (on average 3.6 groups per macrocycle), hydroxypropyl β-cyclodextrin MS 0.6 (on average 4.2 groups per macrocycle), and hydroxypropyl γ-cyclodextrin MS 0.6 (on average 4.8 groups per macrocycle). The solid-state properties of combinations of these derivatives with naproxen were examined using differential scanning calorimetry, which is able to evaluate the crystalline component(s) of a solid mixture, in combination with X-ray powder diffractometry. Dissolution tests (dispersed amount and rotating disc methods) were also performed on drug/carrier mixtures with the aim of showing possible implications of solid-state interactions on the dissolution rate of naproxen. Lastly, since dissolution can also be influenced by drug-cyclodextrin interactions in the liquid state, the solution behaviour of naproxen was investigated with each hydroxypropyl derivative tested for solid-state interactions. Computer-aided molecular modelling was used to supplement the results from phase-solubility studies as regards thermodynamic parameters and the geometry of the inclusion complexation of naproxen with hydroxypropyl cyclodextrins.

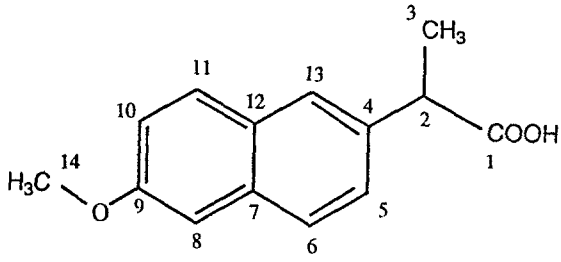

2. Experimental

2.1. MATERIALS

Naproxen (NAP, see structure) (Sigma Chemical Co, St. Louis, MO, USA) and the hydroxypropyl derivatives of α-, β-, and γ-cyclodextrin with average substitution degrees per anhydroglucose unit (MS) of 0.6 (kindly donated by Wacker-Chemie GmbH, Munich, Germany and hereafter abbreviated to HPαCd, HPβCd, and HPγCd respectively) were used. Water contents of the amorphous hydroxypropyl cyclodextrins (HPCds), determined by thermogravimetric analysis (see section 2.4), ranged from 7 to 9% (as mass fraction). All other materials and solvents were of analytical reagent grade.

2.2. SURFACE AREA DETERMINATIONS

Surface area determinations were performed with a Flowsorb II2003 Surface Area Analyser (Micromeritics, Georgia; USA) following the B.E.T. single-point method [7]. Samples were outgassed under a flux of argon/nitrogen 7/3 mixture at 70 °C for 4 h, and the surface area determined by measuring the volume of nitrogen absorbed

by the sample kept in liquid nitrogen was 0.64, 0.91, 0.86 and 0.85 $m^2\ g^{-1}$ for NAP, HPαCd, HPβCd, and HPγCd, respectively.

2.3. PREPARATION OF NAP/HYDROXYPROPYL CYCLODEXTRIN SYSTEMS

Blends of NAP and each hydroxypropyl cyclodextrin (HPCd) tested were prepared by mixing equimolar amounts of drug (75–150 μm granulometric fraction) and carrier (75–150 μm granulometric fraction) in an agate mortar with a pestle. Ground mixtures were obtained by hand-grinding until no changes in their DSC curves could be detected (see Section 2.4). Colyophilized products were prepared by freeze-drying drug-carrier equimolar blends, dissolved in aqueous ammonia solutions, at -50 °C and 1.3×10^{-2} mm Hg (Lyovac GT2, Leybold-Heraeus). Neither residual ammonia nor any decomposition products of NAP were detected in colyophilized samples. Tablets (1.3 cm in diameter) for rotating disc experiments were prepared by compressing about 300 mg of the NAP/HPCd equimolar blend using a laboratory hydraulic press for KBr discs for IR spectroscopy, at a force (about 2 t) which gave tablets of a surface area of 1.33 cm^2 which would not disintegrate within the test interval (5 min). No lubricant was used.

2.4. THERMAL ANALYSIS

Temperature and enthalpy measurements were performed with a Mettler TA4000 apparatus equipped with a DSC 25 cell (10 K min^{-1}, 30–300 °C) on 5–15 mg samples (Mettler M3 microbalance) in Al pans with perforated lids under static air. Thermogravimetric analysis (TG) was conducted on a Mettler TG 50 apparatus (10 K min^{-1}, 30–300 °C) on 15–25 mg samples in alumina crucibles under a nitrogen atmosphere (10 mL min^{-1}).

2.5. X-RAY DIFFRACTION

X-ray powder diffraction patterns were taken with a computer-controlled Philips PW 1800 apparatus over the 2–40° 2θ range at a scan rate of 1° min^{-1}, using CuK_α radiation monochromated with a graphite crystal.

2.6. DISSOLUTION STUDIES

Dissolution rates of NAP from blends and colyophilized products both at the 1 : 1 drug/carrier molar ratio, and for NAP alone, were determined in water at 37 ± 0.5 °C according to the dispersed amount and rotating disc methods. In the dispersed amount procedure, 100 mg of NAP or NAP-equivalent were added to 300 mL of water, in a 400 mL beaker. A glass three-blade propeller (19 mm diameter) was immersed in the beaker 25 mm from the bottom and rotated (f = 100 min^{-1}). Suitable aliquots were withdrawn with a filter-syringe (pore size 0.45 μm) at the specified times and the NAP concentration was determined by a second derivative

ultraviolet absorption method at 274 nm [6]. The same volume of fresh medium was added to the beaker and the correction for the cumulative dilution was calculated. Each test was repeated four times (coefficient of variation $<1.4\%$). In the rotating disc method, tablets prepared as in Section 2.3 were inserted into a stainless steel holder, so that only one face was exposed to the dissolution medium (150 mL). The holder was then connected to a stirring motor, immersed in a 200 mL beaker and rotated ($f = 100\ \text{min}^{-1}$). At appropriate interval times, samples of dissolution medium were withdrawn and assayed for NAP content as above. Each test was repeated four times (coefficient of variation $<8\%$).

2.7. SOLUBILITY STUDIES

Solubility measurements of NAP were carried out by adding 30 mg of drug to 30 mL of water or aqueous solution of HPCd in the 5 to 100 mmol L^{-1} concentration range, in a sealed glass container which was electromagnetically stirred at a constant temperature (25, 37, or 45 °C) until equilibrium was achieved. An aliquot was withdrawn and the NAP concentration was determined as in Section 2.6. Each experiment was performed in triplicate. The apparent formation constants and the thermodynamic parameters of NAP–HPCd inclusion complexation were calculated from the phase-solubility diagrams according to Higuchi and Connors (see for example Ref. [1]).

2.8. MOLECULAR MODELLING

Analysis and modelling of the structures of NAP-cyclodextrin inclusion complexes were carried out using the INSIGHT 2.2.0 programme (Biosym Technologies [8]). The HPCd derivatives were built up by adding 3, 4, or 5 hydroxypropyl groups to α-cyclodextrin (αCd), β-cyclodextrin (βCd), or γ-cyclodextrin (γCd) as base molecules, respectively. Three patterns of substituent distribution were examined for three-substituted αCd, six for tetra-substituted βCd, and three for pentatsubstituted γCd. NAP was fitted into the Cd cavity in an axial orientation, with the carboxyl group located either at the wide 2,3-hydroxyl side [9] or at the narrow 6-hydroxyl side of the cavity. Each structure was subjected to a process of energy minimization (CVFF force field, DISCOVER 2.9 program [8]), performing iterations to a < 0.05 derivative value. Molecular dynamic simulations were performed at 27 °C (time step 1 fs, equilibrium time 100 fs, step number 10 000). Docking energies were calculated at both −273 °C (rigid molecule) and 27 °C, in the latter case averaging the energies of 51 conformations generated during the dynamic molecular program (5 to 10 ps).

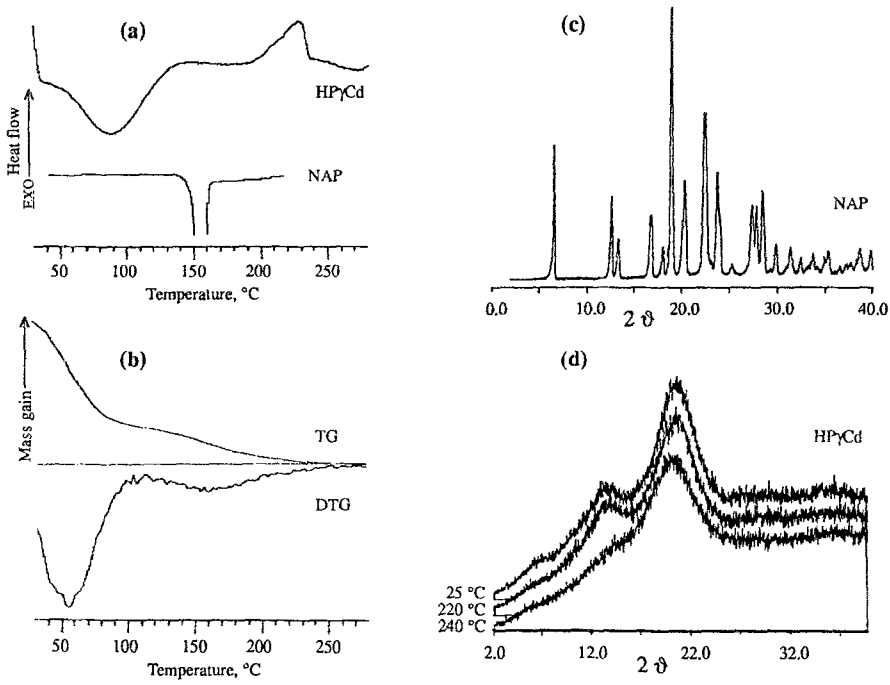

Fig. 1. DSC curves of naproxen (NAP) and hydroxypropyl γ-cyclodextrin MS 0.6 (HPγCd) (a); TG and DTG curves of HPγCd (b); X-ray powder diffraction patterns of NAP (recrystallized from ethanol) (c), and HPγCd kept at room temperature (25 °C) or previously heated to the indicated temperatures (d).

3. Results and Discussion

3.1. SOLID STATE STUDIES

Thermal analysis and X-ray diffraction data indicated the crystalline, anhydrous state of NAP and the amorphous, hydrate nature of each HPCd (Figure 1). After dehydration, noticeable exothermal effects were exhibited by HPαCd (t_{peak} = 228.0 °C, $\Delta_{exo}H$ = 40 J g^{-1}), HPβCd (t_{peak} = 268.7 °C, $\Delta_{exo}H$ = 12 J g^{-1}), and HPγCd (t_{peak} = 226.7 °C, Δ_{exo} H = 44 J g^{-1}, Figure 1a). The phenomenon was more probably due to decomposition than to crystallization of the sample since crystallinity was still absent in the X-ray diffraction patterns of samples that had been previously heated to 220 °C or 240 °C (Figure 1d). TG and DTG curves (Figure 1b) revealed mass losses over two distinct temperature ranges, that between 30 °C and 110 °C (9.1% as mass fraction), which was probably due to water evolution (about 9 water molecules per HPγCd molecule), and that between 110 °C and 250 °C (3.5% as mass fraction), which might account for an exothermal decomposition of the sample.

In the equimolar blends with each HPCd derivative, the DSC fusion endotherm of pure NAP (t_{peak} = 156.1 ± 0.3 °C, $\Delta_f H$ = 134 ± 5 J g^{-1} [10], see Figure

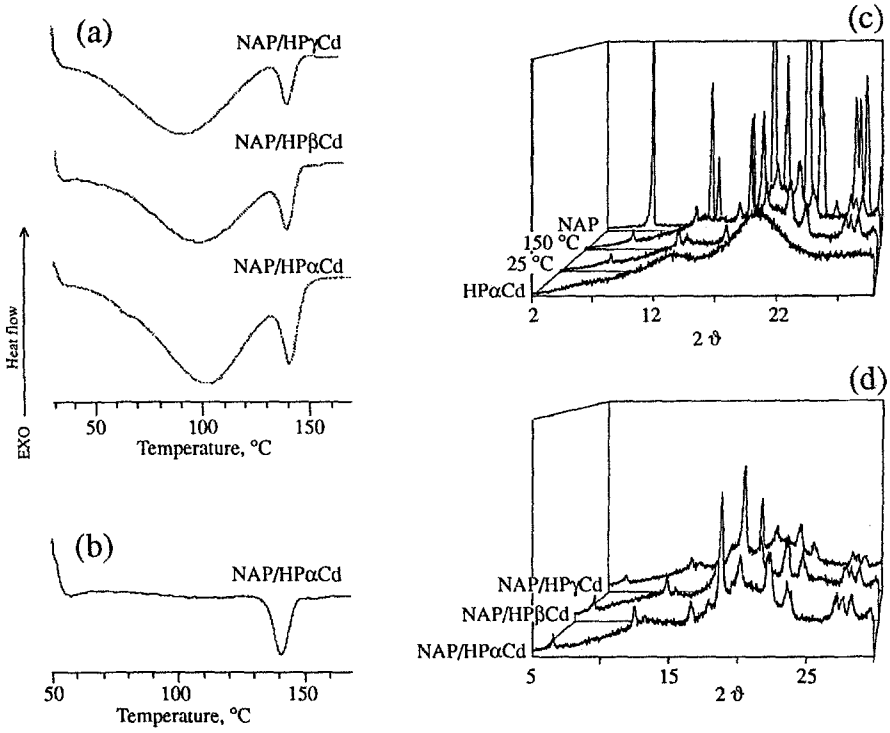

Fig. 2. DSC curves of (a) equimolar blends of naproxen (NAP) with hydroxypropyl cyclodextrin derivatives MS 0.6; (b) NAP/HPαCd equimolar blend after heating to 130 °C and cooling to room temperature in the DSC pan. X-ray powder diffraction patterns of (c) NAP/HPαCd equimolar blend kept at room temperature (25 °C) or heated to 150 °C (150 °C), with those of the pure components; (d) equimolar blends heated to 150 °C (patterns superimposable to those taken for samples kept at room temperature).

1a) peaked at lower temperatures and lay inside the dehydration endotherm of the amorphous carrier (Figure 2a). It was, however, possible to accurately evaluate the fusion enthalpy of NAP in the mixture, and hence its crystallinity, through a thermal cycle where the sample was scanned up to 130 °C, immediately cooled to room temperature and again scanned up to 170 °C, as shown in Figure 2b for the NAP/HPαCd blend. X-ray diffraction patterns showed that the degree of crystallinity of NAP was apparently unchanged when the NAP/HPαCd blend was heated to 150 °C (Figure 2c). The behaviour of the drug in blends with HPβCd and HPγCd was the same (Figure 2d).

DSC analysis of NAP/HPCd blends in various molar ratios showed that the decrease in both peak temperature and area of the drug melting endotherm (i.e., in drug crystallinity) was directly correlated to the mole fraction of carrier present (Table I). The extent of NAP amorphisation was positively influenced by mechanical treatments such as grinding of the mixture, but did not substantially depend on the nature of the carrier, i.e. on the geometrical features of the HPCd macrocycle.

TABLE I. DSC data for blends and ground mixtures of naproxen (NAP) with hydroxypropyl cyclodextrin (HPCd) derivatives MS 0.6 in various molar ratios.

NAP/HPCd (mol/mol)	NAP/HPαCd		NAP/HPβCd		NAP/HPγCd	
	t_{peak}	Crystallinity (%)*	t_{peak}	Crystallinity (%)*	t_{peak}	Crystallinity (%)*
9:1	150.3	87	150.3	91	149.6	89
8:2	146.9	76	148.1	79	145.5	78
7:3	147.0	76	148.0	66	144.4	70
	145.0**	71**	146.3**	64**	143.1**	59**
5:5	146.5	67	148.8	72	146.1	70
	141.3**	54**	143.1**	49**	140.5**	51**
3:7	142.2	52	148.2	67	146.2	50
	139.5**	44**	142.5**	37**	138.5**	44**
2:8	141.2	22	140.5	16	137.8	37

*From specific enthalphy of NAP in the mixture (J/g_{NAP}).
**Values in ground mixtures (see Experimental, 2.2).

3.2. DISSOLUTION RATE AND SOLUBILITY STUDIES

The mean dissolution curves of NAP in dispersed amount experiments are presented in Figure 3a. It is evident at a glance that, as with βCd among native Cds [1], so HPβCd among the derivatives tested was the optimal partner for improving the dissolution rate of the drug. ANOVA in fact showed statistically significant differences ($P < 0.01$) in terms of dissolution efficiency [11] between NAP/HPβCd and both NAP/HPαCd and NAP/HPγCd equimolar blends (Table II). It should be noted that the dissolution performance of the NAP/HPβCd blend was somewhat better than that reported for some NAP/native βCd systems, i.e. kneaded mix, freeze-dried, and spray-dried products [12]. This confirmed the presence in NAP-amorphous HPCds blends of a high-energy state of crystalline NAP, molecularly dispersed in the carrier phase [13]. The dissolution efficiency of the X-ray amorphous NAP/HPβCd equimolar colyophilized product was significantly higher ($P < 0.01$) than that of the respective blend, as expected.

Rotating disc results in terms of dissolution rate constant (k) again showed that HPβCd was the best carrier for NAP, but also a distinct, better performance of HPγCd compared to HPαCd (Figure 3b). A similar trend was observed for NAP/native Cd equimolar combinations, both blended (k = 0.36(2), 1.7(1) and 6.1(9) mg cm^{-2} h^{-1} respectively for α-, γ- and βCd) and colyophilized (k = 1.1(2), 4.7(7) and 8.9(4) mg cm^{-2} h^{-1} respectively for α-, γ- and βCd). The dissolution rate constants of these combinations, however, were noticeably lower than those of NAP/HPCd blends, and this suggested that the high-energy state of crystalline NAP dispersed in the amorphous carrier powder postulated above was maintained after compaction.

TABLE II. Dissolution efficiency* (%) of equimolar solid combinations of naproxen (NAP) with hydroxypropyl cyclodextrin (HPCd) derivatives MS 0.6 (standard deviation in parentheses).

NAP	NAP/HPαCd	NAP/HPβCd		NAP/HPγCd
	blend	blend	colyoph. prod.	blend
7.5(1)	17.1(2)	29.3(4)	46.9(7)	17.1(2)

*Area under the dissolution curve with $t = 60$ min (measured using the trapezoidal rule) expressed as a percentage of the area of the rectangle described by 100% dissolution in the same time [11] (see Figure 3a). Each value is the average of four determinations, coefficient of variation C.V. < 1.4%.

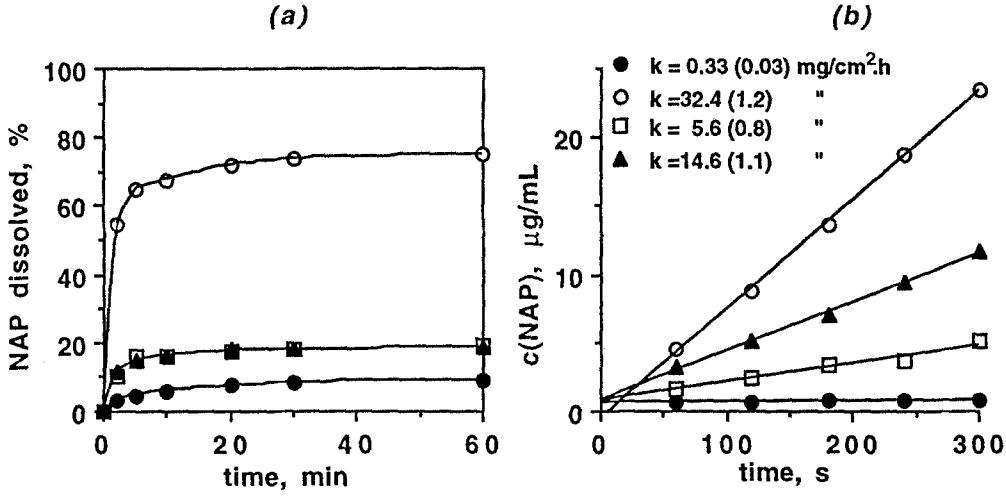

Fig. 3. Mean dissolution curves of naproxen (NAP: ●), its equimolar blends with hydroxypropyl cyclodextrin derivatives MS 0.6 (HPαCd: □ ; HPβCd ○; HPβCd: △) and its colyophilized product with HPβCd MS 0.6 (■). (a): dispersed amount method, 4 runs, coefficient of variation <1.4%; (b): rotating disc method, 4 runs, coefficient of variation <8%.

A_L-type phase-solubility diagrams (Figure 4), and thermodynamic parameters (Table III) reflected the faster drug release rates from NAP/HPβCd combinations, in terms of a specific drug-βCd interaction in aqueous medium characterized by an increase in solvent entropy associated with hydrophobic bond formation [14]. As a result, the 'solubilising efficiency' of HPβCd for NAP was one order of magnitude higher than those of HPαCd and HPγCd (Table III).

3.3. MOLECULAR MODELLING

Computer-generated structures of four NAP–HPCd inclusion complexes are displayed in Figure 5. Van der Waals energy values of docking between NAP (substrate, penetrating the cavity from the wide 2,3-hydroxyl side either methoxy-end

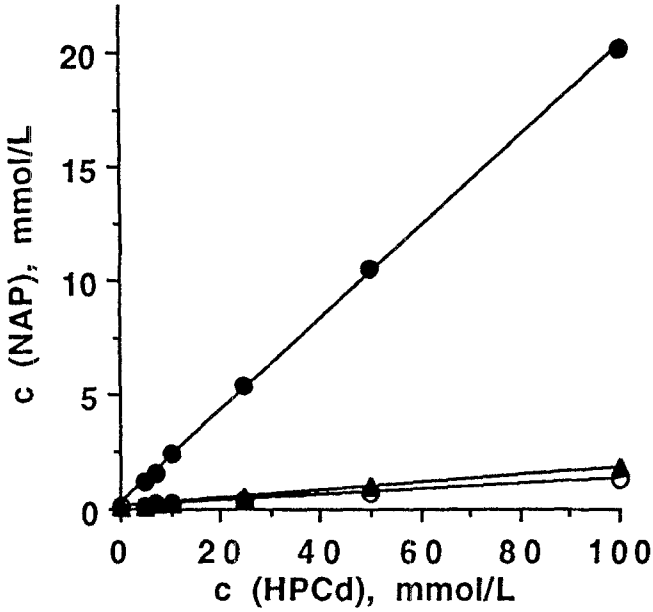

Fig. 4. Phase-solubility diagrams in unbuffered pH ≈ 5 aqueous solution at 25 °C of naproxen (NAP) with hydroxypropyl cyclodextrin derivatives MS 0.6: HPαCd (○), HPβCd (●), HPγCd (▲).

TABLE III. Stability constants and derived thermodynamic parameters for the interaction of naproxen (NAP) with native cyclodextrins (αCd, βCd, γCd) and hydroxypropyl cyclodextrin (HPCd) derivatives MS 0.6 in unbuffered aqueous solution (pH ≈ 5).

Cyclodextrin	Solubilising efficiency*	Apparent stability constant $K_{(1:1)}$ (L mol^{-1})				$\Delta G^{\circ}_{25\,^{\circ}C}$	ΔH°	$\Delta S^{\circ}_{25\,^{\circ}C}$
		25 °C	32 °C	37 °C	45 °C	kJ mol^{-1}	kJ mol^{-1}	J mol^{-1} K^{-1}
αCd	1.3	40	34	20		−9.1	−16.2	−23.8
HPαCd	2.0	103	–	85	60	−11.5	−12.2	−2.5
βCd	14.8	1702	1482	1388	–	−18.5	−13.2	17.6
HPβCd	20.3	2083	–	1726	1694	−18.9	−12.0	23.1
γCd	2.1	146	124	79		−12.3	−17.6	−17.6
HPγCd	2.3	187	–	128	107	−12.9	−13.9	−3.1

*Relative increase in NAP solubility at 25 °C, calculated as the ratio between NAP solubilities in 1×10^{-2} M aqueous solution of cyclodextrin and in pure water.

first or carboxyl group first) and the hydroxypropyl Cd derivative (host) at −273 and 27 °C are summarized in Table IV. Values for docking of NAP with native Cds are also given for comparison purposes. No statistically-significant differences in docking energy values were observed by varying the relative position of substituted glucoses in patterns (a), e.g., 1,3,4 instead of 1,3,5 for HPαCd, or 1,2,4,5,7

instead of 1,3,5,7,8 for HPγCd. The results were the same when a hydroxypropyl group was moved from the primary to the secondary O(2)H hydroxyl group of the same glucose ring (see for example pattern (a′) of HPβCd in Table IV). No statistically-significant differences were obtained either when NAP was docked in the HPβCd models based on the preferential substituent distribution over the βCd macrocycle [5, 6] (patterns (b) and (c) in Table IV). Statistically-significant differences ($P < 0.05$) were instead found when the docking energy values at 27 °C for the NAP-HPCd interactions were compared with those of the respective native Cds. Thus, a more energetically favoured situation (i.e. the formation of a more stable complex) occurred for NAP-HPCds than for NAP-native Cd inclusion complexation. Comparing docking parameters of both native and hydroxypropylated homologous Cds, a trend of molecular modelling to overestimate the interaction energy of NAP with αCd was evident. The relevant interaction energy was expected to be of the same order of magnitude as that of the NAP-γCd interaction, on the basis of thermodynamic parameters calculated from solubility experiments (see Table III). The disagreement could be explained by considering that in these docking experiments the water molecules present in the cavity of the host could not be taken into account due to computational limitations; so that the guest molecule was allowed to deeply penetrate the αCd cavity, thus assuming a more energetically favoured position. Moreover it must be stressed that we arbitrarily chose the three-substituted as a model for HPαCd MS 0.6 (i.e., carrying on average 3.6 groups per macrocycle) rather than the tetra-substituted pattern. As far as the penetration of NAP into the cavity of HPCds is concerned, the differences between the two insertion modes were not statistically significant ($P < 0.05$) (Table IV), that is to say the energies of interaction were similar for either orientation of NAP inside the cyclodextrin cavity.

4. Conclusion

The pharmaceutical usefulness of natural, crystalline Cds can be improved through the transformation by non-specific chemical substitution into multicomponent, amorphous mixtures which are very soluble in water. The improvement is usually seen as an increase in solubility and dissolution rate of drugs, and in this respect both native and hydroxypropylated βCd was undoubtedly the 'tailored partner' for NAP. The ability of amorphous Cds to act as amorphising agents of crystalline drugs and at the same time as stabilising agents for the amorphous state they brought forth cannot be overlooked. It should be noted that amorphisation of NAP occurs when the drug powder is blended with the amorphous carrier, probably as a consequence of loosening of crystal forces of the drug dispersed within the amorphous matrix [6]. No specific surface area effects operate in the solid state interaction between NAP and the HPCds tested since, as in the case of NAP-hydroxyethyl βCd systems [5,6], all the derivatives display substantially the same value of this parameter. The extent of amorphisation depends on the relative amount of carrier

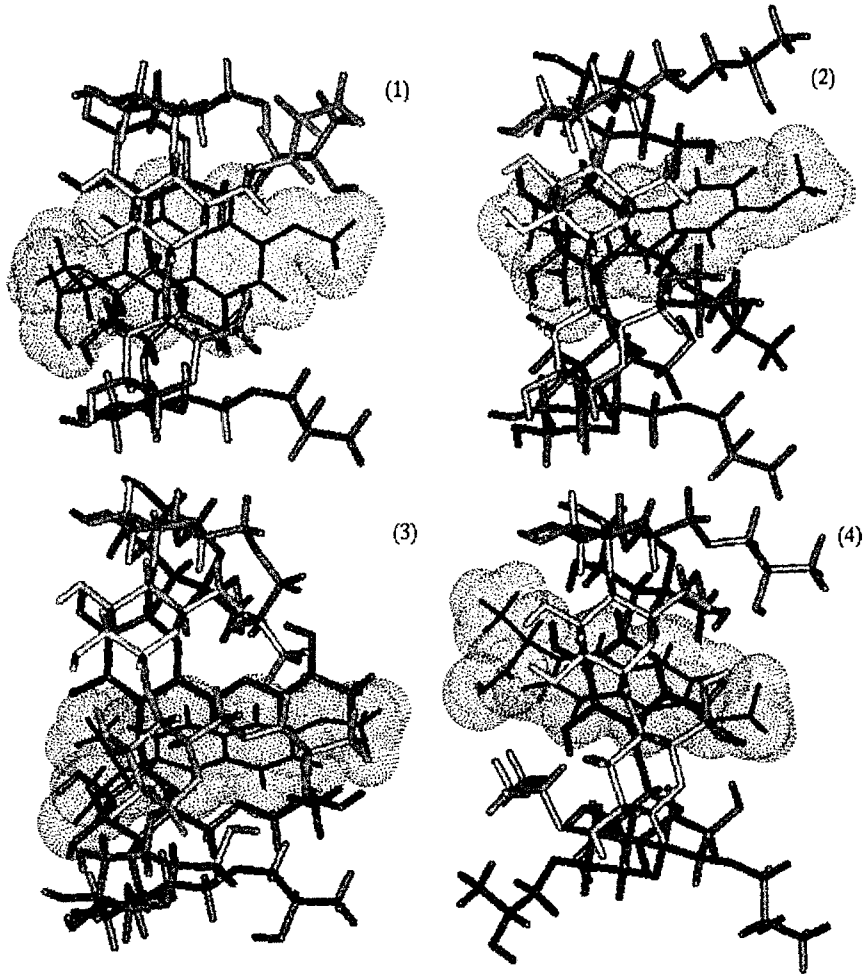

Fig. 5. Computer generated 1 : 1 inclusion complexes between NAP (fitted into the cavity from the wide 2,3-hydroxyl side, methoxy-end first) and model molecules of α-, β-, and γ-hydroxypropyl cyclodextrin derivatives MS 0.6. (1) HPαCd, three substituents on primary OH groups of glucoses 1,3,5; (2) HPγCd, five substituents on primary OH groups of glucoses 1,3,5,7,8; (3) HPβCd, four substituents on primary OH groups of glucoses 1,3,5,7; (4) HPβCd, three substituents on primary OH groups of glucoses 1,3,5, one on the secondary O(2)H group of glucose 7.

present in the mixture, i.e. the higher the carrier mole fraction, the higher the mole fraction of crystalline drug transformed. An important role in this solid-state interaction is also played by the nature of the substituent on the cyclodextrin moiety (e.g., CH_3— > CH_3—CH(OH)— > $HOCH_2$—CH_2— for βCd in the rank order most effective to least [3,4]) and by the average degree of substitution (e.g., MS 1.6 > MS 1.0 > MS 0.6 for hydroxyethyl βCd in the rank order most to least effective [5,6]). The geometrical features of the macrocycle instead seem not to be directly involved in the amorphisation process of NAP, because HPαCd is roughly

TABLE IV. Docking energies* for the interaction of naproxen (NAP) with native cyclodextrins (αCd, βCd, γCd) and some model molecules of hydroxypropyl cyclodextrin (HPCd) derivatives MS 0.6 at −273 °C and 27 °C (standard deviation in parentheses).

Cyclodextrin	Distribution of substituents**	Docking energy (kJ mol^{-1})	
		−273 °C	27 °C
αCd	–	−163	−142(8)
HPαCd	(a) 1,3,5	−181	−163(10)
		−173§	−160(9)§
βCd	–	−149	−140(8)
HPβCd	(a) 1,3,5,7	−182	−150(8)
		−170§	−154(9)§
HPβCd	(a′) 1,3,5,7 (O2)	−180	−149(8)
HPβCd	(b)	−164	−143(9)
HPβCd	(c)	−159	−152(6)
γCd	–	−162	−116(8)
HPγCd	(a) 1,3,5,7,8	−163	−125(7)
		−181§	−133(11)§

*NAP fitted in the cavity from the wide 2,3-hydroxypropyl side, methoxy-end first.
§Values obtained for NAP fitted in the cavity from the wide 2,3-hydroxypropyl side, carboxyl group first (i.e. with its methoxy group oriented towards the widest rim of the cavity).
**(a): substituents at the level of primary OH groups distributed equally between the glucoses; (a′): HPβCd model (a) with substituent on ring 7 moved from the primary O(6)H to the secondary O(2)H hydroxyl group; (b) three substituents clustered on one glucose, the fourth on a primary OH group; (c): substituents forming an oligomeric chain on a primary OH group.

as active as both HPβCd and HPγCd. Grinding produces an increase in the amount of drug which is brought to an amorphous state in the mixture, the increase being in general greater in proportion to the increase in the mole fraction of the carrier present. It should be stressed that the availability of amorphous pharmaceuticals which are adequately stable in the conditions of pharmaceutical processing allow one to overcome the technological problems linked to the intrinsic thermodynamic instability of the amorphous state, which represents the major handicap for practical uses. Molecular modelling concerned Cds carrying a fixed number of substituents per Cd macrocycle, i.e. 3 for HPαCd, 4 for HPβCd, and 5 per HPγCd. Actually there are other components of a random substituted derivative of a native Cd, for example, in the case of HPβCd MS 0.6 tested, those with 3.5 (MS 0.5) and 5 (MS 0.7) substituents per macrocycle. Moreover only a few patterns of substituent distribution on the cyclodextrin macrocycle were considered in docking energy calculations. It remains to be seen if derivatives having a different number

and/or distribution of substituents will have similar or different properties as host molecules for NAP. A trend of molecular modelling data to account for a more stable inclusion complexation of NAP with HPCds than with the respective native Cds is however unquestionable, in agreement with the thermodynamic parameters obtained from solubility experiments. It should be pointed out in conclusion that structural information on the inclusion complexes of NAP with amorphous cyclodextrin derivatives cannot be obtained by X-ray single crystal data, due to their non-crystalline state. Molecular modelling, complemented with NMR data, constitutes a useful approach to this purpose.

Acknowledgements

Financial support from the MURST (fondi 60%) and CNR is gratefully acknowledged.

References

1. G. P. Bettinetti, P. Mura, A. Liguori, G. Bramanti, and F. Giordano: *II Farmaco* **44**, 195 (1989).
2. D. Duchêne and D. Wouessidijewe: *Pharm. Techn. In.* **2**, 21 (1990).
3. G. P. Bettinetti, P. Mura, F. Melani, and F. Giordano: *Minutes 5th Int. Symp. Cyclodextrins* (Ed. D. Duchêne, Ed. de Santé, Paris), pp. 239–242 (1990).
4. G. P. Bettinetti, A. Gazzaniga, P. Mura, F. Giordano, and M. Setti: *Drug Dev. Ind. Pharm.* **18**, 39 (1992).
5. G. P. Bettinetti, P. Mura, F. Melani, and F. Giordano: *Proc. 7th Intern. Cyclodextrins Symp.* (Acad. Soc. Japan, Tokyo), pp. 455–458 (1994).
6. P. Mura, G. P. Bettinetti, F. Melani, and A. Manderioli: *Eur. J. Pharm. Sci.* in press (1995).
7. S. Brunauer, T. H. Emmett, and E. Teller: *J. Am. Chem. Soc.* **60**, 309a (1938).
8. Byosim Technologies, 9685 Scranton Road, S. Diego, CA 92121-2777.
9. G. P. Bettinetti, F. Melani, P. Mura, R. Monnanni, and F. Giordano: *J. Pharm. Sci.* **80**, 1162 (1991).
10. G. P. Bettinetti, P. Mura, F. Giordano, and M. Setti: *Thermochim. Acta* **199**, 165 (1991).
11. K. A. Khan: *J. Pharm. Pharmacol.* **27**, 48 (1975).
12. J. Blanco, J. L. Vila-Jato, F. Otero, and S. Anguiano: *Drug Dev. Ind. Pharm.* **17**, 943 (1991).
13. O. I. Corrigan and C. T. Stanley: *J. Pharm. Pharmacol.* **34**, 621 (1982).
14. R. J. Bergeron, D. M. Pillor, G. Gibeily, and W. P. Roberts: *Bioorg. Chem.* **7**, 263 (1978).